# Black hole scattering: the self-force approach

Chris Whittall

QMUL journal club
25th March 2024

# Talk outline

A) Introduction to self-force

B) Self-force in black hole scattering

C) Frequency-domain appproach

D) Future work

# PART A: Introduction to self-force

**Reviews:**

L. Barack & A. Pound, *Self-force and radiation reaction in general relativity*, 2019 Rep. Prog. Phys. **82** 016904 [arXiv:1805.10385]

E. Poisson, A. Pound & I. Vega, *The Motion of Point Particles in Curved Spacetime*, Living Rev. Relativ. **14**, 7 (2011) [arXiv:1102.0529]

# The 2-body problem in GR: approaches

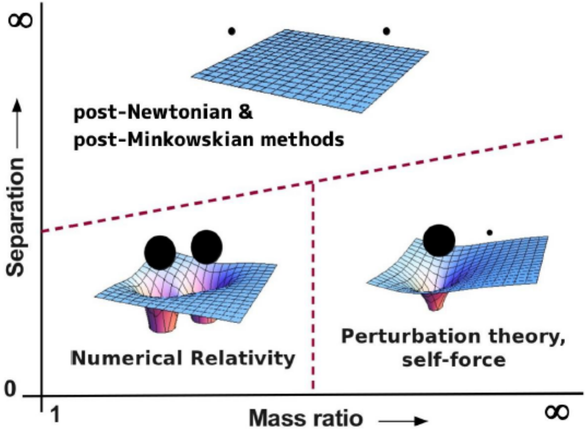


Image credit: L. Barack & A. Pound

# Extreme mass ratio inspirals (EMRIs)

Created using KerrGeodesics package from BHP toolkit.

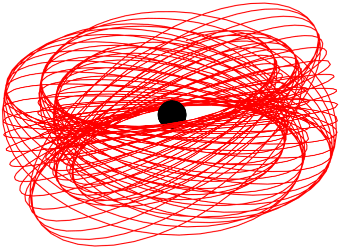

- Highly asymmetric compact binaries. Typical mass ratios

$$q \sim \frac{10 M_\odot}{10^6 M_\odot} = 10^{-5} \ll 1 \quad (1)$$

- Inspiral slow compared to orbital periods:

$$T_{\mathrm{RR}} \sim T_{\mathrm{orb}}/q \gg T_{\mathrm{orb}}. \quad (2)$$

- Large number of gravitational wavecycles in LISA band before merger:

$$N_{\mathrm{orb}} \sim 1/q \sim 10^5. \quad (3)$$

- Orbital dynamics complicated. Geodesics tri-periodic and generically ergodic.
- EMRIs offer a precision prfobe of strong-field geometry around black-holes.

# Self-force expansion

Metric of the physical spacetime is expanded about background as a series in $q := m/M \ll 1$,

$$g^{\mathrm{phys}}_{\alpha\beta} = g_{\alpha\beta} + q h^{(1)}_{\alpha\beta} + q^2 h^{(2)}_{\alpha\beta} + \ldots \tag{4}$$

- 0SF: Background metric $g_{\alpha\beta}$. Smaller object moves along fixed background geodesic.
- 1SF: Perturbation $h^{(1)}_{\alpha\beta}$ sourced by point particle on fixed background geodesic. Leading order conservative and dissipative self-forces $\propto q$.
- 2SF: Perturbation $h^{(2)}_{\alpha\beta}$ sourced by particle on 1SF-perturbed trajectory. Gives rise to additional self-force terms $\propto q^2$.

Particle description derived, not assumed.

# 1SF equation of motion

- Metric perturbation may be split into regular and singular fields, [Detweiler & Whiting 2003]

$$h_{\alpha\beta} = h^{R} + h^{S}, \tag{5}$$

defined in terms of certain acausal Green's functions.

- Only $h^{R}_{\alpha\beta}$ contributes to the self-force. For example, at 1SF order,

$$\frac{Du^{\alpha}}{d\tau} = q\nabla^{\alpha\beta\gamma} h^{R(1)}_{\beta\gamma}\Big|_{z(\tau)} + O(q^2), \tag{6}$$

where

$$\nabla^{\alpha\beta\gamma} h_{\gamma\beta} := -\frac{1}{2}\left(g^{\alpha\beta} + u^{\alpha}u^{\beta}\right) u^{\gamma}u^{\delta}\left(2\nabla_{\delta}h_{\beta\gamma} - \nabla_{\beta}h_{\gamma\delta}\right). \tag{7}$$

# Computational approach: mode-sum regularisation

- Singular field subtracted mode-by-mode in a spherical harmonic expansion around the large BH:

$$F_{\text{self}}(\tau) = m \sum_{\ell=0}^{\infty} \left[ \left(\nabla h^{\text{ret}}\right)^{\ell} - \left(\nabla h^{\text{S}}\right)^{\ell} \right]_{z(\tau)} \tag{8}$$
$$= \sum_{\ell=0}^{\infty} \left[ m \left(\nabla h^{\text{ret}}\right)^{\ell} \Big|_{z(\tau)} - A(z)\ell - B(z) - C(z)/\ell \right] - D(z).$$

- Regularization parameters: derived analytically for generic Kerr orbits. [Barack & Ori 2000-03]

- Numerical input: modes of $h^{\text{ret}}_{\alpha\beta}$ calculated numerically by solving perturbation equations with point-particle source and retarded BCs.

# PART B: Self-force in black hole scattering

L. Barack & O. Long, *Self-force correction to the deflection angle in black-hole scattering: a scalar charge toy model*, Phys. Rev. D **106** 104031 (2022) [arXiv:2209.03740]

L. Barack et al, *Comparison of post-Minkowskian and self-force expansions: Scattering in a scalar charge toy model*, Phys. Rev. D **108** 024025 (2023) [arXiv:2304.09200]

# Scatter orbits

Particle starts at radial infinity at early times with velocity $v$ and *impact parameter* $b$:

$$b = \lim_{\tau \to -\infty} r_p(\tau) \sin |\varphi_p(\tau) - \varphi_p(-\infty)| \,. \tag{9}$$

Provided $b > b_{\rm crit}(v)$, particle scatters off central black hole, approaching to within periapsis distance $r_{\rm min}$.

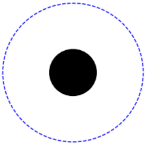

# Why study scattering?

- Theoretical grounds:
  1. Can probe sub-ISCO region even at low velocities; down to light ring $r = 3M$ with large $v$.
  2. Scattering angle $\chi(b, v)$ defined unambiguously, even with radiation.

- Boundary-to-bound relations between scatter and bound orbit observables, derived using effective-field-theory. [Kalin & Porto 2020]

- PM expansion of $\chi$ can be used to calibrate effective-one-body models [Damour 2016].

- $\chi_{\rm 1SF}$ determines **full** conservative dynamics to 4PM, valid at *any* mass ratio. Extend to 6PM with $\chi_{\rm 2SF}$ [Damour 2020].

# Comparisons with PM

- Significant recent progress in PM theory, driven by techniques from outside the usual community (EFT, amplitudes).
- State of the art results at 4PM. [Bern et al 2021 and Dlapa et al 2022]
- Comparisons between PM and SF approaches allow mutual validation. [Barack et al 2023]
- SF results are "exact" i.e. contain PM terms of all orders at given order in $q$. Benchmark PM results in strong-field regime.

# Self-force correction to the scatter angle

- Scatter angle expanded as

$$\chi = \chi^{(0)} + q_s \delta\chi, \tag{10}$$

where $\chi^{(0)}$ is the scatter angle of the geodesic with the same $(b, v)$.

- Correction expressed as integral over the worldline, [Barack & Long 2022]

$$\delta\chi = \int_{-\infty}^{+\infty} A_\alpha(\tau; b, v) F^\alpha(\tau) d\tau. \tag{11}$$

At $O(q)$, integral may be evaluated along limiting geodesic.

- Can split into conservative and dissipative pieces using orbital symmetries:

$$F_\alpha^{\rm cons}(r, \dot{r}_p) = -F_\alpha^{\rm cons}(r, -\dot{r}_p), \quad F_\alpha^{\rm diss}(r, \dot{r}_p) = F_\alpha^{\rm diss}(r, -\dot{r}_p) \quad (\alpha = t, \varphi). \tag{12}$$

# Scalar-field toy model in Schwarzschild

- Toy model: scalar charge $Q$ with mass $m$ moving in a background Schwarzschild spacetime of mass $M$:

$$\nabla^\mu \nabla_\mu \Phi = -4\pi Q \int_{-\infty}^{+\infty} \frac{\delta^4(x - x_p(\tau))}{\sqrt{-g(x)}} d\tau. \tag{13}$$

- Scalar-field calculation captures the main challenges of gravitational self-force calculations, in a simpler overall framework.

- Parameter $q_s := Q^2/(mM) \ll 1$ takes the role of the mass ratio.

- First numerical calculations by [Barack & Long 2022] using time domain numerical approach.

# Scalar-field self-force

- Equation of motion: 4-momentum $mu^\alpha$ evolves according to

$$\frac{D}{d\tau}(mu^\alpha) = Q\nabla^\alpha\Phi^R. \tag{14}$$

- Component parallel to $u^\alpha$ controls mass variation:

$$\frac{dm}{d\tau} = -Q\frac{d\Phi^R}{d\tau} \implies m(\tau) = m^{\text{rest}} - Q\Phi^R(\tau). \tag{15}$$

- Projection orthogonal to $u^\alpha$ defines the scalar-field self-force:

$$m\frac{Du^\alpha}{d\tau} = Q\left(\delta^\alpha_\beta + u^\alpha u_\beta\right)\nabla^\beta\Phi^R =: mq_s F^\alpha. \tag{16}$$

# Early scatter angle results [Barack & Long 2209.03740]

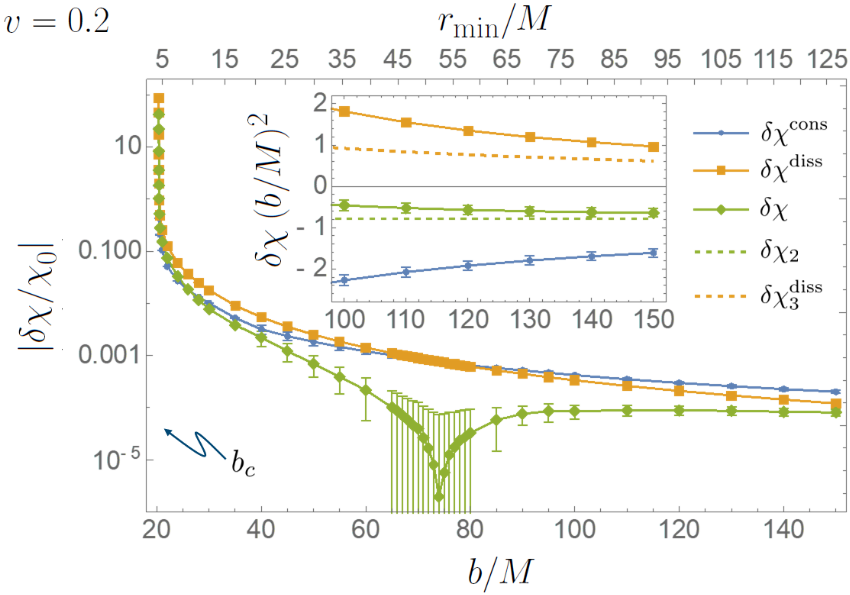

# Scalar-field self-force in terms of amplitudes

- Action:

$$S = \int d^D x \sqrt{-g}\Big[-\frac{2}{\kappa^2}R + \frac{1}{2}\phi_1(\Box + m_1^2)\phi_1 + \frac{1}{2}\phi_2(\Box + m_2^2)\phi_2 + \frac{1}{2}\psi\,\Box\,\psi + \boxed{\frac{1}{2}Q\psi\phi_1^2}\Big]$$

  $\phi_{1,2}$ black holes, scalar field $\psi$.

- 3-point vertices:

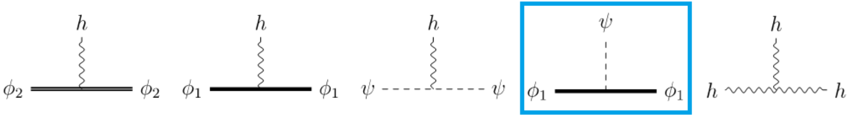


- Keep terms which are linear in mass-ratio and proportional to $Q^2$

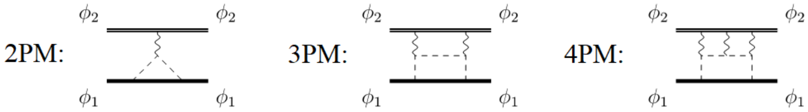


[Cheung, Rothstein, Solon] [Bern, Cheung, Roiban, Shen, Solon, Zeng]

[Bern, Cheung, Para-Martinez, Roiban, Ruf, Shen, Solon, Zeng]

# PM comparisons [Barack et al 2304.09200]

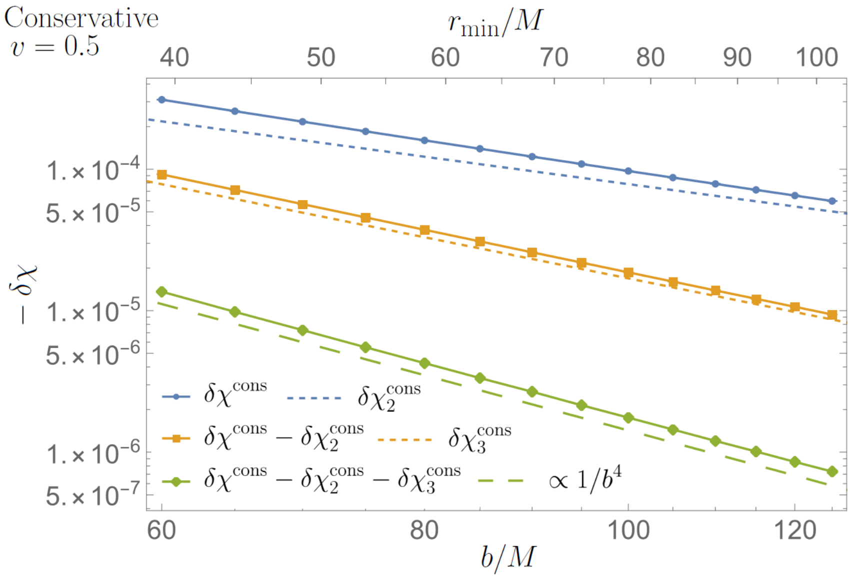

# PM comparisons [Barack et al 2304.09200]

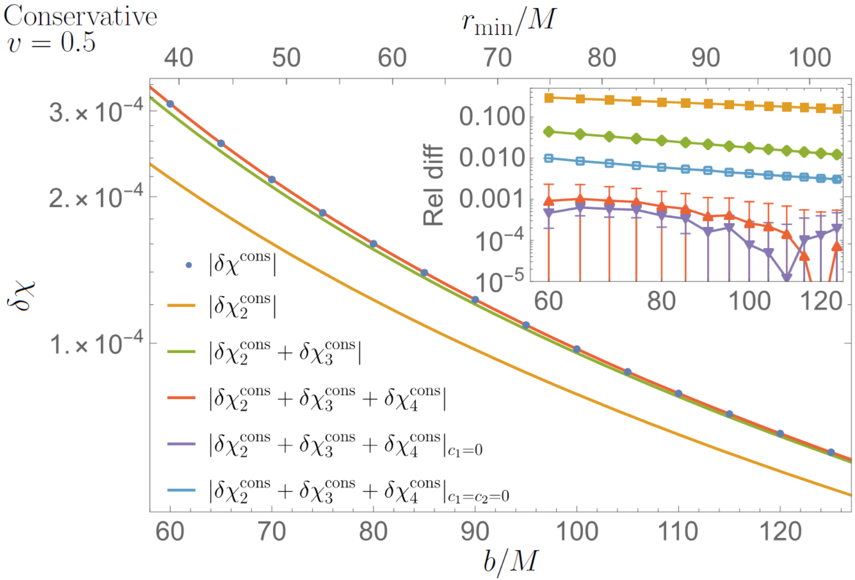

# PART C: Frequency-domain approach

C. Whittall & L. Barack, *Frequency-domain approach to self-force in hyperbolic scattering*, Phys. Rev. D **108** 064017 (2023) [arXiv:2305.09724].

# Frequency-domain methods

- Fields are decomposed into spherical and Fourier harmonics, e.g.

$$\Phi(t, r.\theta, \varphi) = \frac{1}{r} \sum_{\ell=0}^{\infty} \sum_{m=-\ell}^{\ell} Y_{\ell m}(\theta, \varphi) \int_{-\infty}^{+\infty} d\omega \, \psi_{\ell m \omega}(r) e^{-i\omega t}. \quad (17)$$

- Many frequency-domain (FD) self-force codes in existence for bound orbits. Valued for their accuracy and efficiency.

- FD methods expected to retain these advantages when moving to unbound orbits, but challenges must be overcome:
  - Continuous spectrum.
  - Failure of EHS method.
  - Slowly convergent radial integrals.
  - Cancellation during TD reconstruction.

We use a scalar-field toy model in Schwarzschild to investigate and manage these problems.

# Scalar-field toy model

- Field equation becomes

$$\frac{d^2\psi_{\ell m\omega}}{dr_*^2} - \left[V_\ell(r) - \omega^2\right]\psi_{\ell m\omega} = S_{\ell m\omega}(r). \tag{18}$$

- Admits homogeneous solutions $\psi^{\pm}_{\ell\omega}(r)$ obeying retarded BCs at either horizon or infinity. Retarded inhomogeneous solution constructed using variation of parameters:

$$\psi_{\ell m\omega}(r) = \psi^{+}_{\ell\omega}(r)\int_{r_{\min}}^{r}\frac{\psi^{-}_{\ell\omega}(r')S_{\ell m\omega}(r')}{W_{\ell\omega}f(r')}dr' + \psi^{-}_{\ell\omega}(r)\int_{r}^{+\infty}\frac{\psi^{+}_{\ell\omega}(r')S_{\ell m\omega}(r')}{W_{\ell\omega}f(r')}dr' \tag{19}$$

- Gibbs phenomenon: impractical to reconstruct SF modes from physical solution $\psi_{\ell m\omega}(r)$.

# Extended homogeneous solutions [Barack, Ori & Sago 2008]

- Method of Extended Homogeneous Solutions restores exponential, uniform convergence.

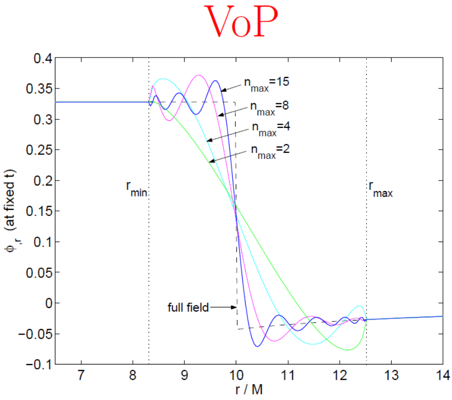


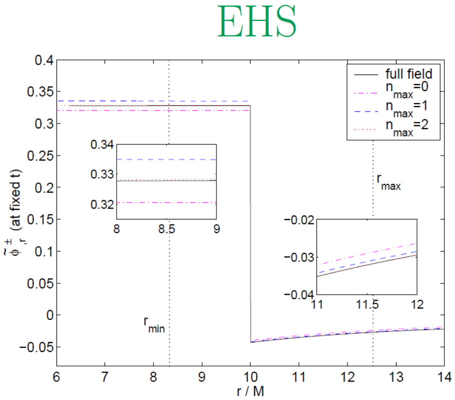

# Extended homogeneous solutions

- Physical time-domain field is reconstructed piecewise from **homogeneous** solutions. For example, SF modes in the "internal" region $r \leq r_p(t)$ reconstructed from

$$\tilde{\psi}^{-}_{\ell m\omega}(r) := \psi^{-}_{\ell\omega}(r) \int_{r_{\rm min}}^{+\infty} \frac{\psi^{+}_{\ell\omega}(r') S_{\ell m\omega}(r')}{W_{\ell\omega} f(r')} dr'. \tag{20}$$

- In vacuum region $r \leq r_{\rm min}$, this EHS field coincides with the physical, inhomogeneous field. Continue to all $r \leq r_p(t)$ in the time-domain.

- For unbound orbits, EHS cannot be used to reconstruct field in the "external" region $r > r_p(t)$.

We use EHS and one-sided mode-sum regularisation

# Truncation problem

- Need to evaluate the **normalisation integrals**,

$$C^{-}_{\ell m\omega} := \int_{r_{\min}}^{+\infty} \frac{\psi^{+}_{\ell\omega}(r')S_{\ell m\omega}(r')}{W_{\ell\omega} f(r')} dr', \tag{21}$$

which stretch over the (unbounded) radial extent of the orbit.

- Slow, oscillatory convergence: problems when truncated at finite $r_{\max}$.
- Developed solutions:
  1. Tail corrections: use large-$r$ approximation to integrand to derive analytical estimates to the neglected tail.
  2. Integration by parts (IBP): use IBP to increase decay rate of integrand.

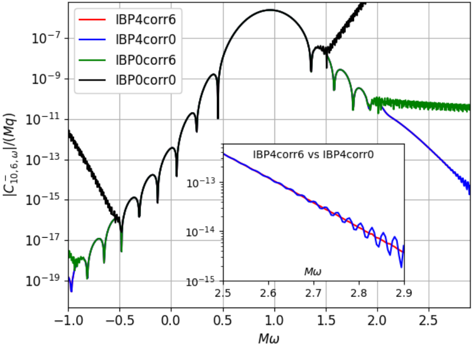

# $C^{-}_{\ell m\omega}$ spectra

Example $C^{-}_{\ell m\omega}$ spectra for orbit $E = 1.1$, $r_{\min} = 4M$. Note QNM features.

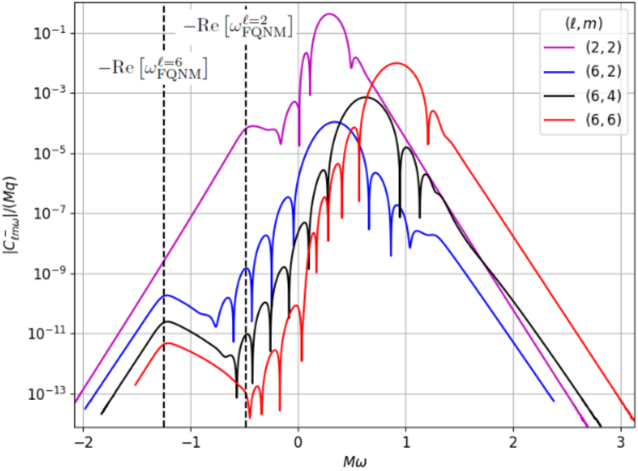

# Self-force: regularisation tests

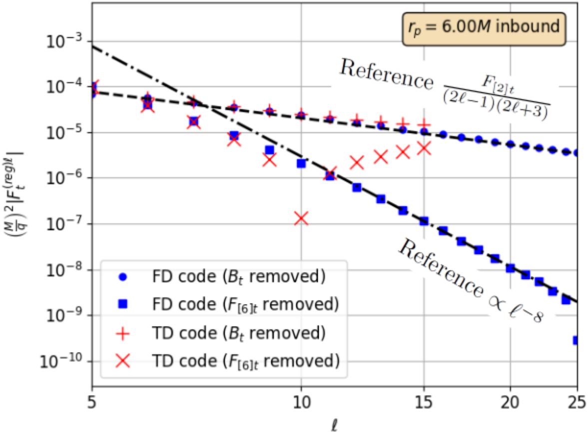


$E = 1.1, r_{\rm min} = 4M.$

FD code agrees better with regularisation parameters at this radius

$$F(\tau) = \sum_{\ell=0}^{\infty} \left[ q \left(\nabla \Phi^{\rm ret}\right)^{\ell} \Big|_{z(\tau)} - A(z)\ell - B(z) - C(z)/\ell - H.O.P \right] - D(z)$$

# Cancellation problem

- Significant cancellation between low-frequency modes at large $\ell$ and $r$.
- Caused by unphysical growth of the EHS field.
- Problem intrinsic to EHS approach. Afflicts scatter calculations more severely than bound orbit case.

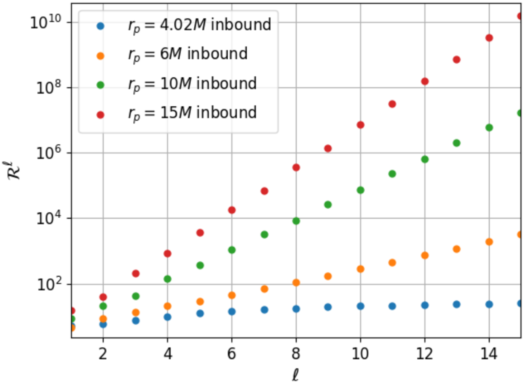


Partially mitigate using dynamic $\ell$-truncation in the mode-sum.

# Self-force: along orbit

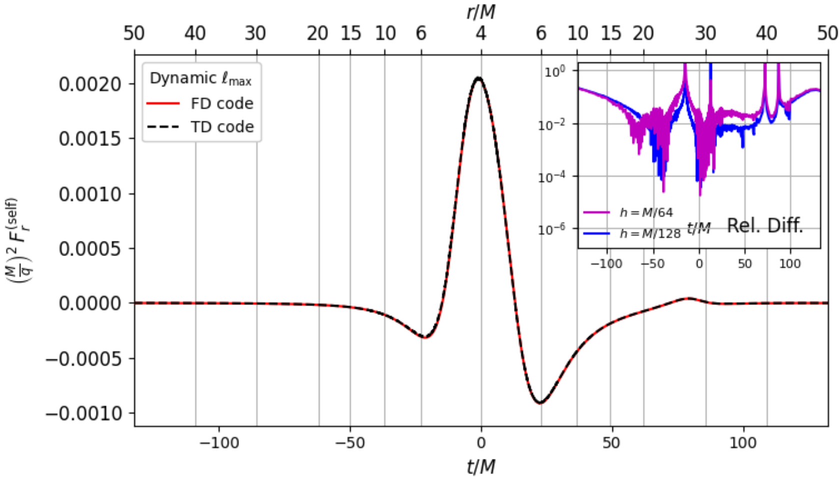


Gradual loss of accuracy along orbit due to progressive loss of $\ell$-modes.

# PART D: Future work

# Analytical calculation: overview

- Want analytical expressions for scalar-field/self-force as $t \to \pm\infty$ as an expansion in $1/r_p$:
  1. Supplement FD code at large radii.
  2. Supplement TD codes, evolve over shorter periods.
  3. Provide initial conditions to TD evolutions, reducing junk radiation.
  4. Large-$r$ tails in scatter angle integrals.

- Makes use of a hierarchical expansion, [Barack 1998]

$$\psi_{\ell m}(u,v) = \sum_{N=0}^{\infty} \psi_N(u,v), \tag{22}$$

$$\psi_{0,uv} + V_0(r)\psi_0 = S(u,v), \tag{23}$$

$$\psi_{N,uv} + V_0(r)\psi_N = -\delta V(r)\psi_{N-1} \quad (N>0), \tag{24}$$

where $V_0(r)$ approximates asymptotic behaviour of exact potential $V(r)$, and $\delta V(r) := V(r) - V_0(r)$.

# Analytical calculation: $\psi_0$ order (preliminary)

$$\psi_0(u,v) = \int_{-\infty}^{u} du' \int_{-\infty}^{v} dv' \; G(u,v;u',v') S(u') \delta(v' - v_p(u')) \tag{25}$$

- Leading order piece $\sim 1/r_p^2$:
  - Calculation complete.
  - Does not contribute to SF (confirmed analytically).
  - Initial comparisons to numerical data promising.

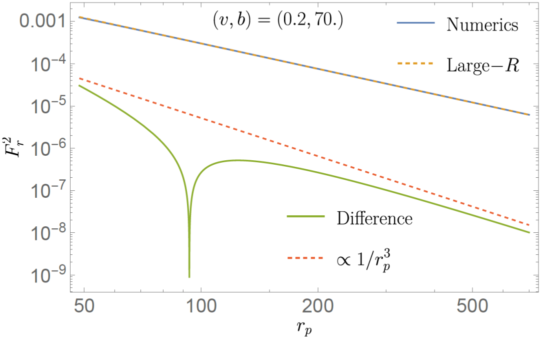


- Next-to-leading order piece $\sim 1/r_p^3$:
  - Calculation incomplete.
  - Expect NLO orbit terms to contribute to the leading-order SF.

# Analytical calculation: $\psi_1$ order (preliminary)

Multiple integration with 2 Green's functions:

$$\psi_1(x) = -\int_{-\infty}^{u} du' \int_{-\infty}^{v} dv' \; G(x;x')\delta V(r')\psi_0(x') \tag{26}$$

$$= -\int_{-\infty}^{\tilde{u}(u,v)} du'' \int_{u''}^{u} du' \int_{v_p(u'')}^{u} dv' \; G(x;x'), \delta V(r') G(x'; u'', v_p(u''))S(u'')$$

where $x := (u, v)$ etc., $\tilde{u} = u$ for $v \geq v_p(u)$ and $\tilde{u} = u_p(v)$ for $v < v_p(u)$.

- Leading order piece $\sim 1/r_p^3$:
  - Contributes to leading-order SF.
  - Integral divided into many sections - many do not contribute.
  - Calculation ongoing.

# PM resummation

- Divergence: as $b \to b_c(v)$,

$$\chi_{0\mathrm{SF}} \sim A(v) \log\left(1 - \frac{b_c(v)}{b}\right) + const(v); \quad \delta\chi_{1SF} \sim q_s B(v) \frac{b_c(v)}{b - b_c(v)}. \tag{27}$$

  where $A(v)$ known analytically and $B(v)$ is extracted numerically.

- Introduce

$$\Psi^{\mathrm{nPM}}(b, v) := A\left[\log\left(1 - \frac{b_c(v)(1 - q_s B/A)}{b}\right) + \sum_{k=1}^{n} \frac{1}{k}\left(\frac{b_c(v)(1 - q_s B/A)}{b}\right)^k\right]. \tag{28}$$

- 1SF-resummed scatter angle

$$\tilde{\chi}^{\mathrm{nPM}}(b, v) := \chi^{\mathrm{nPM}}(b, v) + \Psi^{\mathrm{nPM}}(b, v). \tag{29}$$

  Matches *nPM* result in $b \to \infty$ limit, and 0SF and 1SF divergences as $b \to b_c(v)$.

- Similar to geodesic order approach in [Damour & Rettegno 2023].

# 1SF resummation: results (preliminary)

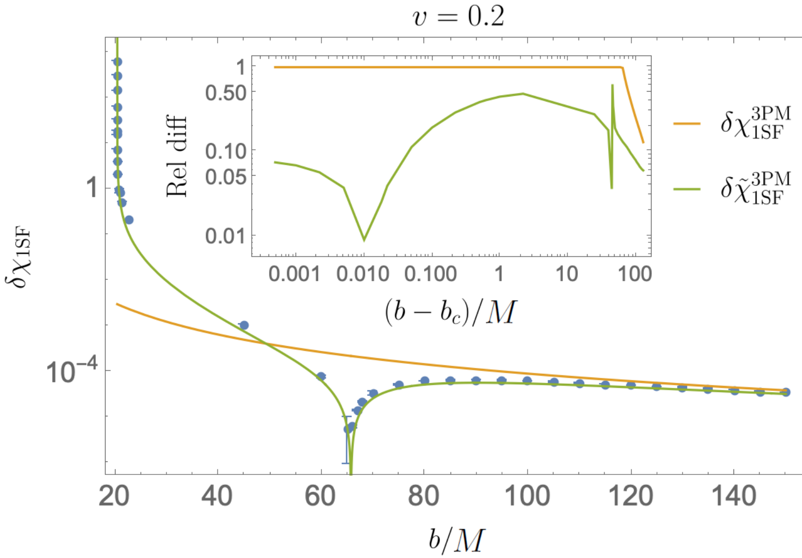

# 1SF resummation: results (preliminary)

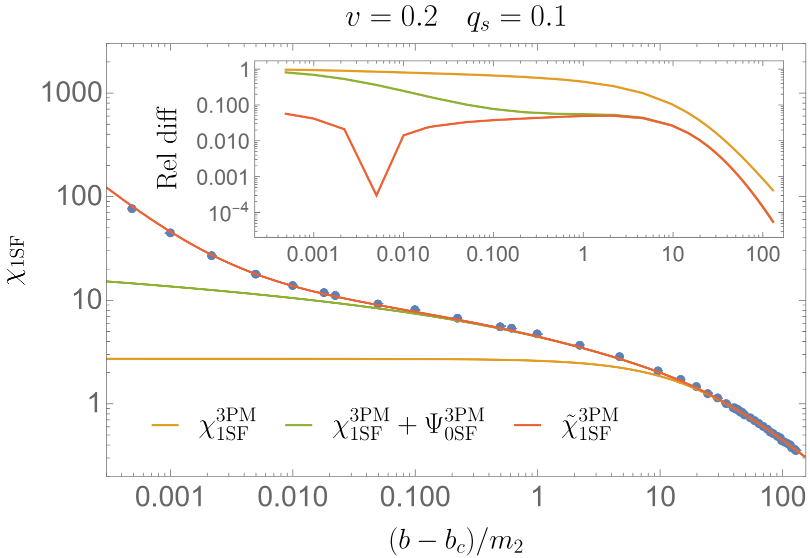


Improvement compared to geodesic resummation.

# PM resummation: additional developments (preliminary)

- **High velocities:** large-$\ell$ modes become more important at higher velocities.
  - Possibly related to relativistic beaming of radiation.
  - Effect strongest near periapsis.
  - FD code can get $\ell \geq 15$ modes near periapsis.
  - Developing FD/TD hybrid method.

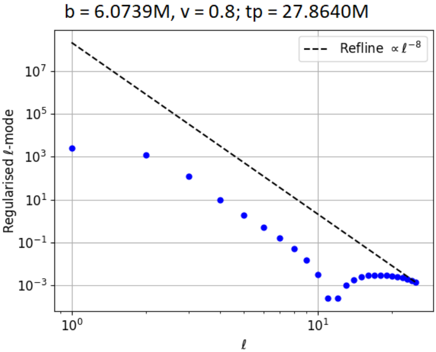


- **Direct approach**: express $B(v)$ as integral over critical orbit, $b = b_c(v)$.
  - Only need to calculate SF along critical orbit. More accurate and efficient than fitting.
  - Numerical methods need some modification e.g. for FD must handle distributional piece of spectrum arising from asymptotic circular orbit.

# Prospects

- Analytical results for SF at large $r$: useful for both TD and FD approaches.

- Improved TD methods also under development, including spectral methods with hyperboloidal slicing and compactification.

- Routes to gravity?
  - Direct Lorenz-gauge calculation [Ackay, Warburton, Barack 2013]
    - → Investigated extending h1Lorenz package to unbound orbits with Warburton and Barack.
  - Radiation-gauge reconstruction [Pound, Merlin, Barack 2013]
  - Lorenz-gauge reconstruction [Dolan, Durkan, Kavanagh, Wardell 2023]

- Second order?
  - Easier than bound? No disparate timescales.
  - Would give conservative dynamics to 6PM.
  - Some way off.